# Form finding and design of a timber shell-nexorade hybrid

Romain Mesnil, Cyril Douthe, Tristan Gobin, Olivier Baverel

AAG2018
**Advances in Architectural Geometry 2018**
Chalmers University of Technology
Gothenburg, Sweden
22-25 September 2018

www.architecturalgeometry.org/aag18

# Form Finding and Design of a Timber Shell-Nexorade Hybrid

Romain Mesnil, Cyril Douthe, Tristan Gobin, Olivier Baverel

## Abstract

The aim of this paper is to discuss the form-finding of an innovative structural system through the design and construction of a full-scale timber pavilion. Nexorades, or multi-reciprocal grids, are structures where members support each other along their spans. This structural principle allows simple assembly and connection details, but leads in counterpart to poor structural performance. Introducing planar plates as bracing components solves this issue, but result in a complex and intricate geometry of the envelope and supporting structure. This paper discusses the different challenges for the designers of shell-nexorade hybrids and algorithmic framework to efficiently handle them in a project workflow.

**Keywords** Nexorade, Shell-nexorade hybrid, timber structure, marionette technique

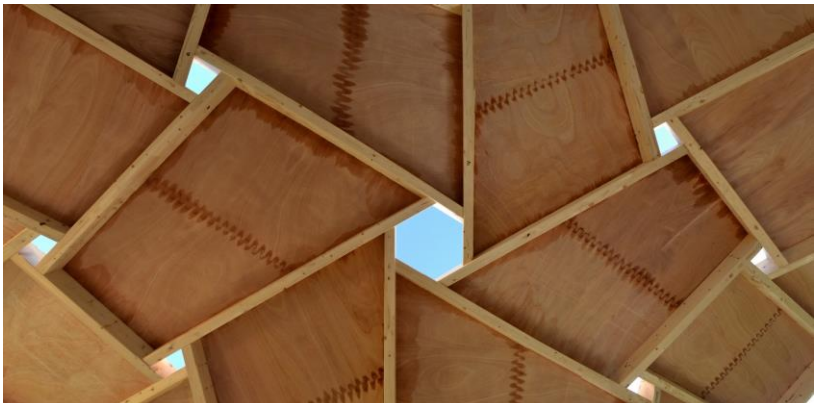

**Fig. 1** The central fan of the pavilion

# 1 Introduction

Nexorades, also known as reciprocal frames or multi-reciprocal grids, are structures constituted of short members which supports on their ends. They are simple to assemble because of they avoid the construction of complex connection details and can be built with short members. For that matter, they have been used since medieval architecture, for example by Villard de Honnecourt, or in sketches of Leonardo da Vinci in the Codex Atlanticus (Bowie 1960). Recent examples of nexorades include the 'Plate Pavilion' in Malta, the 'KREOD Pavilion', designed by architect Chun Qing Li, engineers Ramboll and geometry consultants Evolute, and timber nexorades in ETH Zürich (Kohlhammer, et al. 2017).

Despite their ease of assembly, the structural behavior of nexorade is far from optimal, because of the low valence, which implies a bending-dominated behavior, even for funicular shapes (Brocato 2011). This has been observed in the material science community, where this property of nexorades is used to create auxetic materials. In structural engineering, this behaviour limits the range of spans where those structure are economical and efficient. The structural behavior of nexorades can however be improved by bracing them with planar quadrilateral panels. The authors call 'shell-nexorade hybrids' the new resulting structural system.

The handling of both facet planarity and of the geometry of nexorades at the same time is unexplored up to now, and requires tailor-made geometrical algorithm for construction-aware structural form finding. This paper discusses thus a dialectic approach between constructive geometry and structural mechanics and its application to the form-finding and construction of a timber pavilion, shown in Figure 1.

# 2 Structural and fabrication requirements

In engineering practice, optimization or rationalization have multiple competing objectives and constraints. When aiming at high slenderness, structural detailing and envelope detailing merge, so that the fabrication process and structural design process intertwine. The design of the pavilion is driven by the structural and fabrication constraints, which are described in this section.

## 2.1 Project description

The project aims at illustrating the potential of shell-nexorade hybrids as an efficient and easy-to assemble structural system. First, we have to introduce some vocabulary specific to nexorades. Nexorades are constituted of load-bearing members, which support each other along their span and not their

extremities. The generation of their geometry is based on the displacement of edges of a watertight mesh. The displacements create engagement windows, shown in thick blue lines in Figure 2. Two values characterize the engagement windows: their lengths, called engagement lengths, and the eccentricity, which is the distance between the neutral axis of two concurrent members.

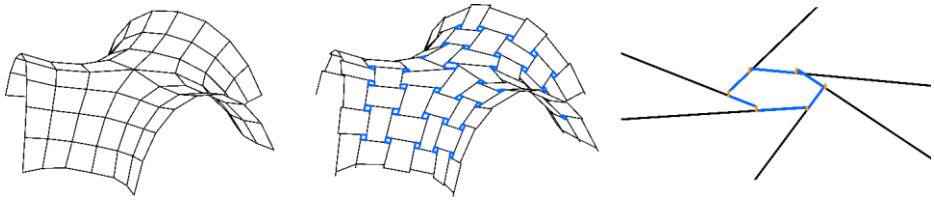

**Fig 2** The reference geometry (left), a nexorade resulting from a transformation of the mesh with engagement windows in blue (middle), a close-up on a fan: the engagement length is the length of a blue line, while the eccentricity is the distance between the lines, highlighted in orange (right).

The pavilion is constructed with cross-laminated timber beams and 10mm thick plywood panels. The pavilion has a span of approximately 7 meters and covers an area of 50m². Its shape is inspired by the CNIT, a thin shell supported on three punctual supports: the geometry and pattern topology allow to build by cantilevering from a central tripod. The beams weigh approximately 5 kilograms and can be assembled in-situ by two people. Mechanical attachment, as opposed to chemical attachments, are used to guarantee on-site assembly. With a thickness of 14cm, the slenderness ratio is of 50, a rather high value for timber structures.

## 2.2 Fabrication and construction requirements

Fabrication constraints are induced by the robotic fabrication process, the materiality of timber and by structural considerations. The panels covering the structure must be as planar as possible, in order to guarantee their fabrication from plywood and to avoid coupling between bending and axial forces, as they are used as a bracing system.

The detailing chosen for the connection of beams and panels is shown in Figure 3: beams are connected with end-grain screws, while beam/panel attachment is made by screws. Tenons and mortises are milled in the beams for the assembly process. Grooves are milled in the timber beams as alignment failsafe between panels and beams. The top surface of the beams are milled in order to avoid timber exposure created by the eccentricities. The higher the eccentricity, the less material after milling, and the lower the lever arm and resistance of the connection. The detailing implies thus to minimize the eccentricities, a rather unusual optimization target in nexorades.

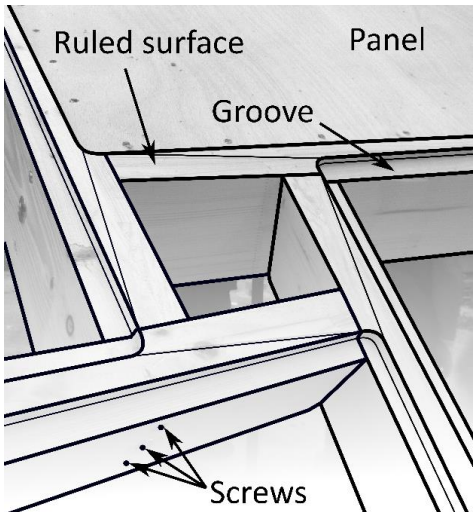


**Fig. 3** A fan during construction showing the detailing: beams are connected by end-grain screws which create a moment-rigid connection, grooves are made in the beam to fit planar panels, and ruled surfaces are milled on top and bottom of the members to avoid timber exposure.

The beams are fabricated with the aid of 6 axes robots shown in Figure 4: one robot on a track with a gripper that is used as a mobile frame for the beam and the other to perform the milling operations. Since the milling of the beam is performed with 13 (6+6+1) axes, the complexity of the attachment between beams and panels can be treated with the milling of the beam. The plates are thus cut with simple 2.5 axes CNC machines. Their width of 1030mm sets constraints on the bounding box of the panels. Other geometrical constraints are imposed by the robotic fabrication process: the size of the gripper imposes a minimal length of 750mm between two mortises, while vibrations restricted the beam length to 2000mm. The speed of cut was adjusted to avoid vibration and to minimize cutting forces. Angles between members also had to be minimized in order to ease the approach of the robotic arms.

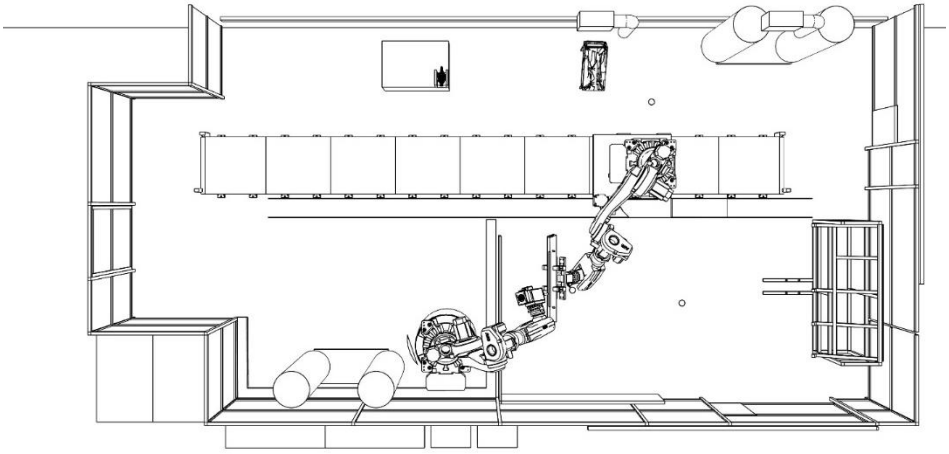

**Fig 4** Top view of the robotic cell with gripping robot on track, milling robot (bottom) and fixed tools (top).

## 2.3 Structural requirements

The structure presented in this paper is a temporary building with a lifespan of one year. As such, it has to withstand climatic and accidental loads. The envisioned accidental load is a non-symmetrical load of 700kg (approximately 10 people climbing on the structure). The loads and design capacity of beams have been derived from the Eurocode 1 and 5 respectively. The connection details, which use end-grain screws, are not designed within Eurocode, and a European Technical Approval (European Technical Approval ETA-11/0190) must be used. The serviceability and ultimate strength requirements are defined as follows:

$$\begin{cases} \delta_{\max} < \frac{L}{300} \\ f\left(\mathrm{N}, \mathrm{V}_y, \mathrm{V}_z, \mathrm{M}_x, \mathrm{M}_z\right) < 1 \end{cases} \quad (1)$$

Where L is the span (6.5m), $\delta_{\max}$ is the maximal deflection under SLS load combination, f is a convex function defined by the technical agreement of the screws describing the utilization of the connection details. Buckling was also checked, but, due to the relatively small span, it is not the governing phenomenon. The ULS design is conservative because not a single nodal failure is allowed.

The final structure weighs approximately 15kg/m², so that self-weight is far from being the governing load case for a temporary building, where creep can be

neglected. Therefore, the geometry does not have to follow a funicular shape, and CAD tools can be used to generate a structural shape. Real-time feedback from a finite element analysis is therefore necessary to optimize the structural behaviour (Bletzinger, Kimmich et Ramm 1991). The reference geometry was thus generated as a collection of NURBS.

## 2.4 Computational workflow

The fabrication and structural requirements are integrated in a computational workflow is presented in Figure 5. The workflow is based on several optimization algorithms that solve construction problems and allow to iterate on the different design parameters to improve the performance of the design. We focus here on the geometrical aspects of the computational workflow, treating the robotic setup as a design constraint. In reality, iterations between the design and the organization of the fabrication platform have been made to guarantee the constructability of the pavilion. It is very likely that an industrial with different machines would have another set of design constraints.

Two levels of geometrical complexity are handled through the design. In early design stages, the architect and engineer deal at a coarse level, called ‘design geometry’ in the flowchart: the members and plates are represented by lines and surfaces respectively, and a priori cross-section are used. This allows to discard bad designs and to quickly iterate and ‘optimize’ the design, although some modelling assumptions are up to the knowledge of the designer. Then, the designer needs to work at a finer level of detail and thus to generate the ‘fabrication geometry’. At this stage, beams are generated as BREP, the proper cross-sections are assigned according to the as-built geometry. The feasibility of the fabrication is also assessed, in our case with the aid of HAL (Schwartz 2012). This step is much more resource demanding, as a considerable amount of fabrication data has to be generated.

The main geometrical operations performed for the form finding of the pavilion aim at complying with the main fabrication constraints. First, the designer sets an input geometry, it is then fitted by a mesh with planar facets. This mesh is then transformed with a custom algorithm, so as to create a nexorade with planar panels. The different fabrication data can then be generated and the structural response is evaluated. The next section discusses in detail these design steps.

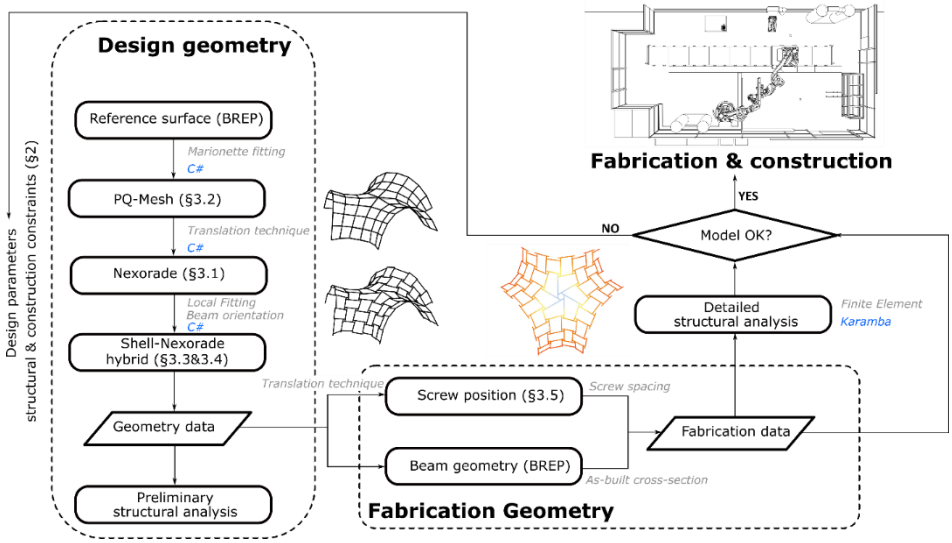


**Fig 5** Computational workflow

# 3 Construction-aware form finding

## 3.1 Form finding of nexorades with the translation method

The form-finding of shell-nexorade hybrid is based on translations of the members, as initially proposed by Baverel (Baverel 2000) and as illustrated in Figure 6. The method takes a mesh as input, the edges correspond either to the neutral axis of the member or the member apex. The geometrical object resulting from the translation of the mesh edges is a collection of lines, which are non-concurrent in general. The translation technique is based on the fact the eccentricity between two lines varies linearly with the translation components (Mesnil, Douthe, et al., Form-finding of nexorades with translation technique 2018). As such, nexorades can be form-found by solving linear least square problems, in the manner of what has been done for polyhedral meshes (Poranne, Chen et Gotsman 2015).

The simplicity of the problem is not surprising, although it has not been noticed before: indeed, edge translations appear in polyhedral mesh modelling. Transformations that preserve edge orientation also preserve facet planarity, and create a linear subspace for shape modelling (Pottmann, et al. 2007) (Poranne, Chen et Gotsman 2015). As a consequence, if the input mesh has planar facets, the nexorade created with the translation technique can be covered with nearly planar panels, although the designer has to deal with eccentricities (distance between the non-concurrent neutral axes of the beams).

The translation technique allows to cover nexorades with planar panels, which can be used as a bracing system. The authors call *shell-nexorade hybrid* the resulting structural system. The practical generation of the structural layout requires first to generate a mesh with planar facets, and then to optimally fit a panel in order to accommodate eccentricities.

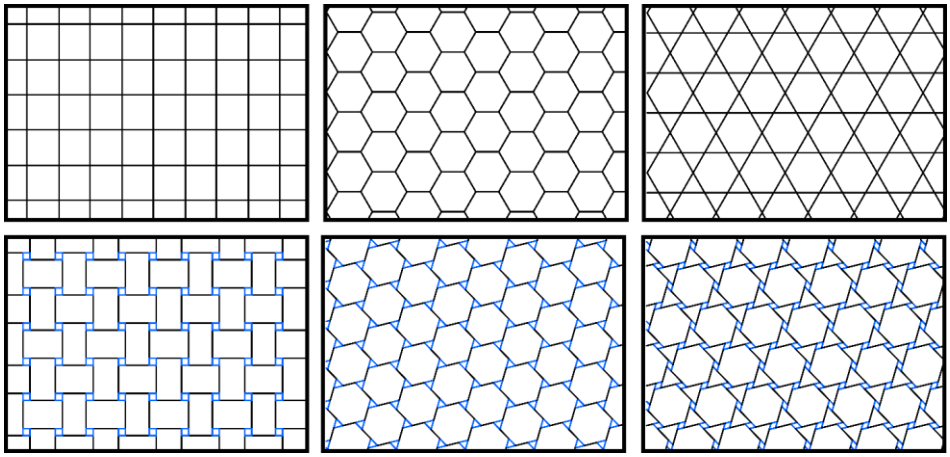

**Fig 6** Some planar tiling (top) and associated nexorade patterns created by edge translation (bottom)

## 3.2 Shape-fitting problem

The input geometry is fitted with the marionette technique, which considers a projection of the mesh as an input, in our case, the plane view, leaving only the altitudes of the mesh vertices as design variables. The technique allows to express the planarity constraint with a linear equation. Additional positional constraints are imposed to some nodes for a better control of the shape, and are also linear.

$$\begin{cases} \mathbf{A}.\boldsymbol{X} = \mathbf{0} \\ \mathbf{B}\boldsymbol{X} = \boldsymbol{C} \end{cases} \tag{2}$$

The matrix $\mathbf{A}$ encodes the planarity constraint for the facets, as described in (Mesnil, Douthe, Baverel, & Léger, Marionette Mesh: from descriptive geometry to fabrication-aware design, 2016). The matrix $\mathbf{B}$ is a sparse matrix, the only non-zero coefficients $\mathrm{B}_{\boldsymbol{ij}}$ are so that the i$^{\text{th}}$ node has the altitude $C_j$. The two constraints can be assembled by stacking the matrices A and B in columns. The optimization becomes a linearly constrained linear least square problem.

$$\min_{\left[\begin{matrix}\mathbf{A}\\ \mathbf{B}\end{matrix}\right].\mathbf{X}=\left[\begin{matrix}\mathbf{0}\\ \boldsymbol{C}\end{matrix}\right]} (\boldsymbol{X}-\boldsymbol{X_t})^T.(\boldsymbol{X}-\boldsymbol{X_t}) \tag{3}$$

The solution of the problem is classical, but recalled here for the sake of completeness. The constrained problem is easily solved with the aid of Lagrange multipliers $\boldsymbol{\lambda}$: optimal values $\boldsymbol{X}^*$ and $\boldsymbol{\lambda}^*$satisfy following linear equation.

$$\begin{bmatrix} 2.\boldsymbol{I_n} & \begin{bmatrix}\mathbf{A}\\ \mathbf{B}\end{bmatrix}^T \\ \begin{bmatrix}\mathbf{A}\\ \mathbf{B}\end{bmatrix} & 0 \end{bmatrix}.\begin{bmatrix}\mathbf{X}^*\\ \boldsymbol{\lambda}^*\end{bmatrix} = \begin{bmatrix} 2.\boldsymbol{X_t} \\ \begin{bmatrix}\mathbf{0}\\ \boldsymbol{C}\end{bmatrix}\end{bmatrix} \tag{4}$$

In practice, the system is solved by performing Cholesky decomposition of the symmetrical matrix on the left-hand side. Few position constraints are chosen so that the problem is not over-constrained, and the matrix of the left-hand side remains invertible. This guarantees the feasibility of the solution using Cholesky decomposition. The solution is fast, even for large number of facets (Sorkine et Cohen-Or 2004).

## 3.3 Mesh planarization

The transformation of a mesh into a nexorade introduces eccentricities, as illustrated in Figure 7, where the end the members are highlighted with black dots (notation $\mathbf{P}^+_i$) and the corresponding closest point on the attached member is highlighted in white (notation: $\mathbf{P}^-_i$). We write $\mathbf{t_i = P}^-_i - \mathbf{P}^+_i$.

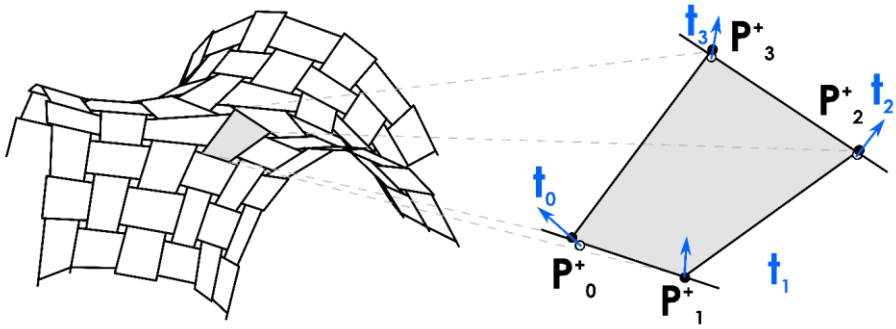


**Fig 7** The form-found nexorade as a collection of lines and the local planarization problem

With the geometry of Figure 7, the designer does not deal with a watertight mesh anymore and must fit envelope panels to the beams and wants thus to minimize following quantity:

$$\sum_{i=0}^{N} \|\boldsymbol{P_i} - \boldsymbol{P_i^+}\|^2 + \|\boldsymbol{P_i} - \boldsymbol{P_i^-}\|^2 \tag{5}$$

With a planarity constraint and the additional design restriction:

$$\boldsymbol{P_i} = \boldsymbol{P_i^+} + a_i.\boldsymbol{t_i} \quad (6)$$

This optimization is a specific example of the marionette technique, with non-parallel lines and is also expressed as a linearly constrained least square problem (Mesnil, Douthe, Baverel, & Léger, Marionette Mesh: from descriptive geometry to fabrication-aware design, 2016). Each equation can be solved independently for each facet. This makes the computation extremely fast and reliable.

In order to better understand why eccentricities arise from the transformation into a nexorade pattern when constructing with planar facets, one can count the degrees of freedom imposed by the planarity and member straightness. We write $n_e$ and $n_v$ the number of edges and vertices in the nexorade, as shown on the bottom of Figure 6. Each edge of a nexorade pattern contains four nodes, except at the boundaries (see bottom of Figure 6), so that $n_v \sim 2n_e$, in addition there are $4n_e$ alignment constraints in the whole nexorade patterns. For two-dimensional nexorade patterns (for example in the XY plane), there are initially $2n_v$ degrees of freedom and $2n_e$ alignment constraints. The estimation of the number of degrees of freedom for nexorade patterns without eccentricities is thus given by equation (7).

$$\begin{cases} d_{3D} \sim 6n_e - 4n_e = 2n_e \\ d_{2D} \sim 4n_e - 2n_e = 2n_e \end{cases} \quad (7)$$

The dimensions of the design spaces are similar, and differ slightly in practice essentially because of “free” borders (where some members have less than four nodes). When adding planarity constraints on the facets (the number of constraints is proportional to the number of facets ), one over-constrains the design space of eccentricity-free nexorade patterns and is left only with nexorade patterns inscribed in a plane. The complexity of milling operations mentioned in this article is thus not a limitation of the proposed form finding technique, but rather an intrinsic limitation of nexorades.

## 3.4 Beam orientation

In timber structures, rectangular cross-sections are commonly used. It is therefore preferable to build torsion-free beam layouts, i.e. to find beam orientation where the beam central plane meet along a common axis. The solution for this problem is not obvious for quadrilateral meshes, but three valent meshes always admit constant face offsets (Pottmann, et al. 2007).

For nexorades, the offsetting problem can easily be solved, because there are only three-valent connections (from a combinatorial point of view), but two-valent connections from a technological point of view: any choice of beam discrete normal yields a torsion-free beam layout. Figure 5 illustrates this statement and the notations for orientation of the beams and panels. The letters Y and Z describe the local material frame corresponding to the strong and weak axis respectively.

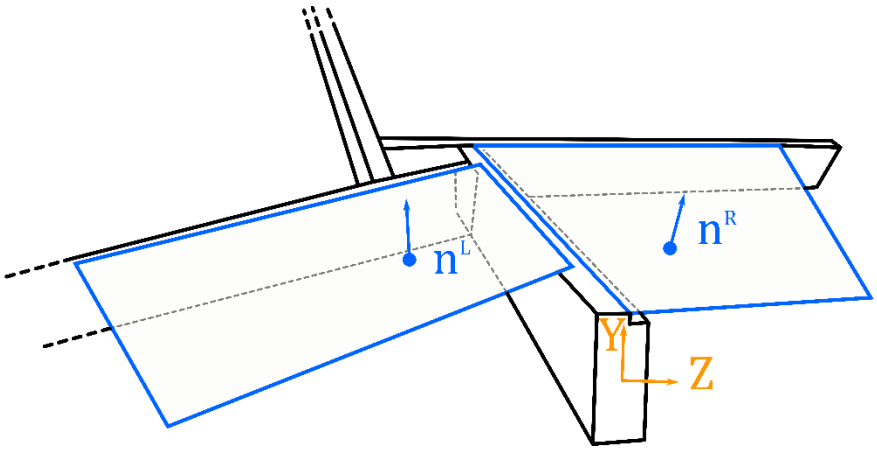


**Fig 8** Notations for the orientations of beams and panels

We can define the normal as the bisector vector between the adjacent faces normal, as shown in equation (8).

$$\boldsymbol{Y_i} = \left(\boldsymbol{n_i^L} + \boldsymbol{n_i^R}\right) - \left(\boldsymbol{n_i^L} + \boldsymbol{n_i^R}\right).\boldsymbol{t_i} \quad (8)$$

This choice minimizes the maximal angle between a panel and its supporting beams, which is a constraint in the chosen fabrication set-up. Indeed, as shown in Figure 9, a robot mills the groove for the assembly between beam and panel: large angles can lead to collisions between the tools or robots.

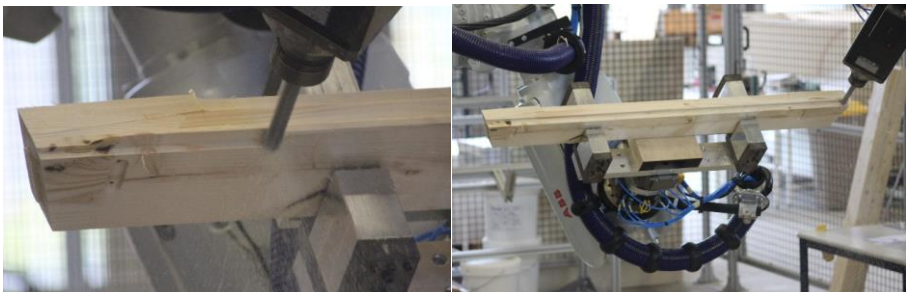

**Fig. 9** Groove milling for panel/beam attachment.

## 3.5 Optimization of connection details

The choice of structural connection details depends on mechanics and assembly. End grain screws are used in the pavilion because they are simple to assemble and do not constrain the assembly kinematics. Details using connecting plates in the timber could not be implemented due to the small width of the members (60mm), but could be used if high structural performance is required. Their main limitation is however the restriction of assembly kinematics, which add an new challenge for the construction sequence planning and execution. Fire safety can also be an issue if the plates are exposed to fire. Glued connections are another alternative with good mechanical performance, but are not suited for in-situ assembly, and do not fit the design requirements of the project. End-grain connections are thus a good alternative to more conventional connections. Moreover, the forces in the connectors are limited in shell-nexorade hybrid, so that yield of connections is a lesser design issue than in classical nexorades, and their lower mechanical performance is not as critical as in other timber structures. Nonetheless, they yield some difficulties for the detailed planning, which are discussed in this section.

The end-grain screwed connections are subject to practical limitations, illustrated in Figure 10: the distance between the screw axis and the beam boundary should remain inferior to 24mm, while the distance between screws should be superior to 24mm. For some fans, the engagement length is inferior to the screw length (200mm), meaning that some collisions between screws might occur: as a result, the position of the screw must be adjusted.

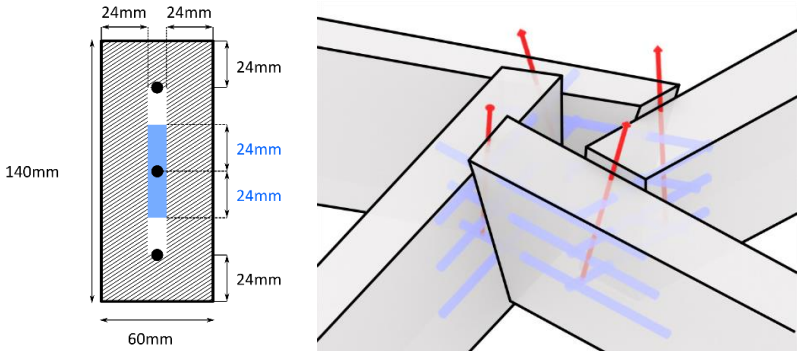

**Fig. 10** Geometrical constraints for the screws layout. Left:Admissible position for screws (white area), and minimal spacing between screws (blue area). Right: a nexor where the screws are longer than the engagement length and potential intersections between them.

The designer aims at maximizing the distance between the top and bottom screws, as it increases the lever-arm, and thus resistance of the connection detail. This must be done without collisions between the screws. This is therefore a constrained optimization problem: the screw layout must be collision-free and respect the bounding box shown on the left of Figure 10. The parameters of the problem are the position of the neutral axes in the local plane of the in-coming beam: the screws can be moved along the red arrows drawn in Figure 10. The screws have a determined orientation: they are aligned with the beam neutral axis. Just like in the form-finding of nexorades by translations presented in Section 3.2, the distance between two screws depends linearly on the amplitude of the translation. The optimization problem of equation is thus a linear programming problem. Fortunately, this problem is not highly coupled: the optimization problem can be solved for each fan separately with the simplex method.

# 4 Structural behavior of shell-nexorade hybrids

## 4.1 Modelling assumptions and design iterations

The structure is modelled with the finite element technique, in order to assess the structural response under non-symmetrical loads. In the preliminary structural design, the cross-section was set to 120mmx60mm, assuming that 20mm of static height at most would be milled because of the eccentricities. This conservative assumption allowed to quickly iterate over the geometry without calculating the beam cross-section after milling. The plywood plates can be modelled with an isotropic material law with a Young's Modulus of 8GPa. A linear elastic model is computed with Karamba, a finite element software integrated in Rhino/Grasshopper (Preisinger 2013), and it was checked that every connection detail was safe. This ensures that the pavilion satisfies the ultimate limit state, but a better approximation of the collapse load could be given by yield design theory or by a geometrically and materially nonlinear analysis (GMNA).

Design iterations were performed at the level of the design geometry, without generating the final geometry of the members. It allowed to create a shape with a strong curvature that provide geometrical stiffness. It also appeared unsurprisingly that decreasing the engagement length improved the structural response of the structure. A design approach purely driven by the optimization of the structural response would result in reducing the engagement lengths. The engagement lengths of individual fans became thus design parameters once a satisfying geometry was found. The minimization of engagement lengths is limited in practice by two constraints: it widens the bounding box of the panels, and small engagement lengths might result in unreachable areas to insert the end-grain screws. The design iterations had thus to take structural response, fabrication and assembly constraints into account.

## 4.2 Benefits of shell-nexorade hybrids

We propose to assess the benefits of introducing plates as bracing elements by comparing the performance of the as-built geometry and cross-sections for the shell-nexorade hybrid and a nexorade without panels. We assume that the load apply in the same way to both structures. The displacements are significantly lower in the shell-nexorade hybrid, especially for non-symmetrical wind and accidental loads, as seen on the left of Figure 11. Forces are also significantly decreases: the right of Figure 11 shows the utilization factor of timber under wind load alone, as prescribed by the Eurocode 5 (the material class is GL24h). It can be seen that, even without combination factor, some members of the unbraced nexorade are over-stressed. Under ULS combination *1.35G+1.5W*, the utilization factor can go up to 200%, even without considering reduction factor for long term load ($k_{mod}$=0), which is absolutely not conservative. The utilization factor of the beams in the shell nexorade hybrid is approximately ten times lower. The introduction of plates as a bracing system is thus highly beneficial, since forces and displacements are divided by ten, with an additional mass of 30%.

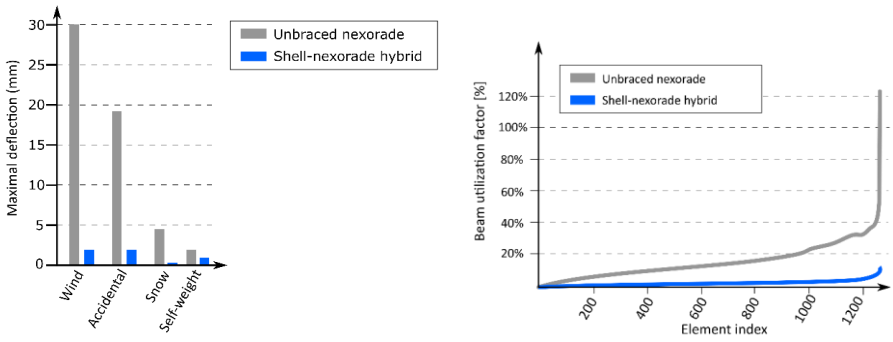


**Fig 11** Displacement under different loads (left) and utilization ratio of beams under wind load alone.

## 4.3 Scalability of nexorades and shell-nexorade hybrid

Different structural systems are available to cover areas with doubly curved structures. This paper focuses on nexorades, or reciprocal systems, and shell-nexorade hybrids. They are easy to assemble and do not require complex connection details. Gridshells are also a classical solution: they are highly efficient, but at the cost of more complex connection details. The relative performances of the different structural systems with respect to the change of scale are assessed in the followings with a simplified comparative study. The geometry of the built pavilion is used as a reference but re-scaled to span larger areas. Then, a sizing optimization is performed under the constraint that the structure satisfies serviceability criterion and ultimate strength criterion, set here to 30% of the characteristic yield strength. The height-over-width ratio of the beams is set arbitrarily to 2.5, and the plates have a thickness-over-span ratio of 100. The only parameter in the sizing optimization is thus the beam width *b*.

$$\begin{cases} \min_{\delta_{SLS}<\delta_d} \; m \\ \sigma_{ULS}<0.3\sigma_k \end{cases} \tag{9}$$

The results of the sizing optimization for different spans are shown in Figure 12. The connections between beams are assumed to be extremely rigid (more than 10 000kNm/rad), in order to sensitivity to nodal stiffness, an important issue for gridshells. The shell-nexorade hybrid and gridshell follow the same trend: the weight increases linearly with the span for spans superior to 25 meters, while the nexorades follow a power law and are clearly outperformed by the two other structural systems. Notice that the gridshell is lighter than the shell-nexorade hybrids: the plates represent a significant part of the total weight in

shell nexorade hybrids with large spans here. This could be fixed by working on hollow plates, or by using a finer mesh pattern for the shell nexorade hybrid. A precise comparison of gridsells and nexorades should be the topic of a more precise study.

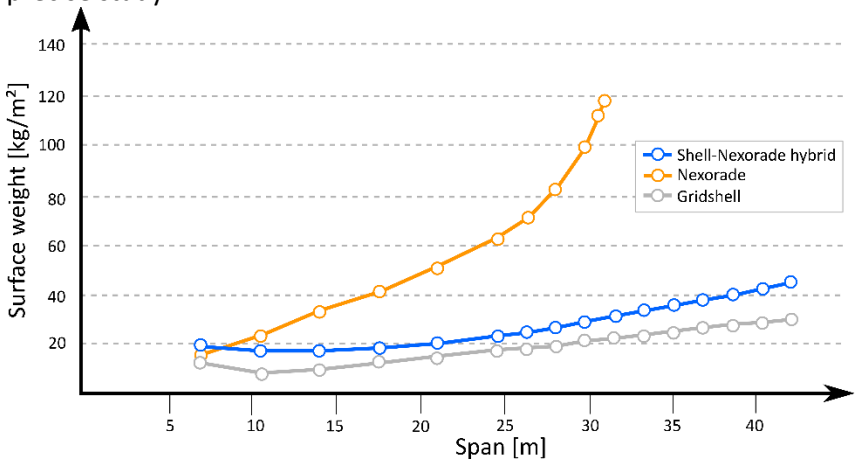


**Fig 12** Influence of the span on the weight of different structural systems.

The trends seen in Figure 12 can be explained with simple arguments. First, it should be noticed that for large spans, the governing load case for the nexorade is self-weight, although the shape is close to a funicular shape.

We explain this trend by considering a cylindrical vault of radius $R$ under uniform load $p$, proportional to the self-weight. We write b,h the width and height of the beams, E the Young's modulus and $\rho$ the volumic mass of timber. An equivalent in-plane membrane stiffness $\mathcal{A}$ can be computed with homogenization techniques, as already done in (Mesnil, Douthe, Baverel, & Léger, linear buckling of quadrangular and kagome gridshells: a comparative assessment, 2017). It has already been observed that the membrane stiffness is proportional to the flexural rigidities of the members, which depends on the $I_2$ and their length $L$, defined as $L * N = R$, where $N$ is the number of subdivisions.

$$\mathcal{A} \propto \frac{EI_2}{L^3} = \frac{Eb^3hN^3}{12R^3} \tag{10}$$

The applied load is proportional to the mass:

$$p \propto \rho bh \tag{11}$$

The meridian force $T$ is given by the classical formula $T = pR$, so that the strain $\varepsilon$ is simply given by:

$$\varepsilon = \frac{\delta}{R} = \frac{T}{\mathcal{A}} \propto \frac{\rho R^4}{Eb^2N^3} \tag{12}$$

The value $\frac{\delta}{R}$ should be limited by a SLS criterion, for example $\frac{\delta}{R} < \frac{1}{300}$. This imposes a condition on the beam width. The proportionality laws derived previously allow to affirm that there exist a factor $k$ so that:

$$b > k\sqrt{\frac{\rho}{EN^3}}.R^2 \tag{13}$$

The height $h$ being proportional to $b$ by hypothesis, one can thus conclude on the trend of the optimal weight for a nexorade that satisfies serviceability under self-weight.

$$p_{opt} \propto R^4$$

The power law observed in Figure 12 does therefore find a simple analytical explanation. However, we observe a strong dependency of the result with respect to the number of subdivision in equation (13). The study presented in this section should thus be further extended to evaluate the influence of subdivision.

The membrane stiffness of gridshells and shell-nexorade hybrids is proportional to the cross-sectional area, which itself is proportional to the surface weight. Thus the sizing optimization under self-weight is scale-invariant, and gridshells and shell-nexorade hybrids are sized with respect to out-of-plane loads.

# 5 Conclusion

Nexorades are structures based on an elegant assembly principle that generally suffer from poor structural behavior. Introducing planar plates as a bracing system opens a new potential of application for nexorades. This paper illustrates the possibilities offered by shell-nexorade hybrids and practical implications of using this new structural principle for fabrication and geometrical modelling. Several optimization problems must be solved to guarantee facet planarity, structural reliance and constructability. The understanding of geometrical properties of nexorades is fundamental in the design workflow. The numerous design iterations are made possible by the flexibility, robustness and speed of the proposed framework and by the handling of geometrical representations of increasing complexity.

A full-scale timber pavilion, shown in Figure 13, was built to validate the methodology proposed in this paper. The structural calculations show that the plates multiply the stiffness by ten with a mass increase by 30%. The pavilion is checked as a temporary building with building codes and technical agreement, so that despite innovations on form finding and fabrication, it has the potential to be proof-checked by an independent engineer. The robotic fabrication within tolerances allowed the manual assembly of the structure with minimal difficulties. Shell-nexorade hybrids combine thus the ease of assembly of nexorades with the stiffness of ribbed shell structures.

**Fig 13** A view of the completed pavilion.

## References


Baverel, O. (2000). *Nexorades: a family of interwoven space structures.* University of Surrey.

Bletzinger, K.-U., Kimmich, S., & Ramm, E. (1991). Efficient modeling in shape optimal design. *Computing Systems in Engineering, 2*(5-6), 483--495.

Bowie, T. (1960). *The sketchbook of Villard de Honnecourt.*

Brocato, M. (2011). Reciprocal frames: Kinematical determinacy. *International Journal of Space Structures, 26*(4), 343-358.

(n.d.). *European Technical Approval ETA-11/0190.*

Flöry, S. (2017). Goat. Rechenraum e.U., Vienna.

Kohlhammer, T., Apolinarska, A., Gramazio, F., & Kohler, M. (2017). Design and structural analysis of complex timber structures with glued T-joint connections for robotic assembly. *International Journal of Space Structures, 32*(3-4), 199-215.

Mesnil, R., Douthe, C., Baverel, O., & Gobin, T. (2018). Form-finding of nexorades with the translation method. *Automation in Construction*, in press.

Mesnil, R., Douthe, C., Baverel, O., & Léger, B. (2016). Marionette Mesh: from descriptive geometry to fabrication-aware design. *Advances in Architectural Geometry* (pp. 62-81). Springer.

Mesnil, R., Douthe, C., Baverel, O., & Léger, B. (2017). linear buckling of quadrangular and kagome gridshells: a comparative assessment. *Engineering Structures, 132*, 337-348.

Poranne, R., Chen, R., & Gotsman, C. (2015). On linear spaces of polyhedral meshes. *IEEE transactions on visualization and computer graphics, 21*(5), 652-662.

Pottmann, H., Liu, Y., Wallner, J., Bobenko, A., & Wang, W. (2007, August). Geometry of multi-layer freeform structures for architecture. *ACM Transactions on Graphics, 26*(3), 6.

Powell, M. (2007). A view of algorithms for optimization without derivatives. *Mathematics Today-Bulletin of the Institute of Mathematics and its Applications, 43*(5), 170-174.

Preisinger, C. (2013). Linking structure and parametric geometry. *Architectural Design, 83*(2), 110-113.

Schwartz, T. (2012). *Rob| Arch* (pp. 92-101). Vienna: Springer.

Sorkine, O., & Cohen-Or, D. (2004). Least-squares meshes. *Shape Modeling Applications* (pp. 191-199). IEEE.